YTUP

Journal of Thermal Engineering
https://jten.yildiz.edu.tr/
https://doi.org/10.47481/jten.0074

RESEARCH ARTICLE

Modeling and CFD analysis of shell-and-tube heat exchanger with helical baffles: performance evaluation through baffle pitch optimization

Dr. G. Maruthi Prasad Yadav[1,*], Mr. G. Md. Javeed Basha[2], Dr. B. Omprakash[3], Mr. E. Madan Manohar[4]

[1]Dept. of Mechanical Engineering, St Johns College of Engineering and Technology, Yemmiganur 518360, AP, India
[2]Dept. of Mechanical Engineering, St Johns College of Engineering and Technology, Yemmiganur 518360, AP, India
[3]Dept of Mechanical Engineering, Jawaharlal Nehru Technological University, Anantapur 515002, AP, India
[4]Central Institute of Petrochemicals Engineering & Technology, Haldia 721657, West Bengal, India

Abstract

This research presents a detailed computational assessment of a shell-and-tube heat exchanger equipped with helical baffles, emphasizing the influence of baffle pitch on the system's overall thermal and hydraulic behavior. The primary aim was to enhance heat transfer capability while limiting pressure losses, which is an essential requirement for industrial sectors such as energy production, petrochemicals, refrigeration, and HVAC (Heating, Ventilation, and Air Conditioning) applications. The heat exchanger model was constructed in CATIA V5, and CFD (Computational Fluid Dynamics) simulations were performed in ANSYS Fluent 15.0 to analyze the impact of different baffle pitches (ranging from 26 to 50 mm) on shell-side performance parameters: pressure drop, temperature difference, and total heat transfer rate over a mass flow range between 0.1571 and 0.6284 kg/s. The computational results found a 38-mm baffle pitch as the most efficient configuration, yielding a maximum heat transfer rate of 14.9 kW and a temperature reduction of 8.4 °C, with a moderate pressure penalty. Visualization of the flow field confirmed the formation of stable swirling and crossflow zones that promote effective mixing without introducing excessive resistance. The study delivers a systematic CFD-based analysis covering a broad range of operating conditions and offers practical guidelines for perfecting industrial heat exchanger designs. The novelty of this work lies in its quantitative evaluation strategy, which decides the best configuration through balanced consideration of both thermal enhancement and fluid dynamic efficiency. In addition to conventional thermal and hydraulic parameters, the study introduces a thermal–hydraulic performance metric based on the heat transfer rate per unit pressure drop($Q/\Delta P$). This index provides an integrated measure of heat transfer effectiveness compared to pumping power. Analysis of this performance index further confirms that the 38 mm pitch delivers the highest thermal–hydraulic efficiency, confirming it as the best configuration across all tested operating conditions.

Keywords: Shell and tube heat exchanger, helical baffles, CFD analysis, baffle pitch optimization

Cite this article as: Yadav, G. M. P., Basha, G. M. J., Omprakash, B., & Manohar, E. M. (2026). Modeling and CFD analysis of shell-and-tube heat exchanger with helical baffles: performance evaluation through baffle pitch optimization. Journal of Thermal Engineering, 12(5), 1915–1928. https://doi.org/10.47481/jten.0074

1. Introduction

Shell-and-tube heat exchangers stay one of the most extensively used configurations in industrial thermal systems, finding applications in sectors such as petrochemical processing, power generation, chemical manufacturing, refrigeration, and HVAC operations. Their widespread adoption stems from advantages such as mechanical robustness, ease of maintenance, design flexibility, and suitability for a broad range of working conditions [1,2,4]. Conventionally, these exchangers employ segmental baffles to direct shell-side flow and augment heat transfer. However, such designs often introduce large pressure losses and vibration-related issues because of the abrupt changes in flow direction along the shell side [7,11].

To overcome these drawbacks, helical baffle designs have appeared as an effective alternative. By inducing a spiral flow path, helical baffles enable smoother fluid motion, reduce

*Corresponding Author
E-mail Adress: maruthiprasadyadav@gmail.com

Submitted: 21 June 2025; **Accepted:** 27 November 2025

This paper was recommended for publication in revised form by Editor-in-Chief Ahmet Selim Dalkılıç

Published by Yıldız Technical University, İstanbul, Türkiye
This is an open access article under the CC BY-NC license (http://creativecommons.org/licenses/by-nc/4.0/).

pressure drop, and enhance heat transfer through improved mixing and extended contact between the fluid and heat transfer surface [2,5,13]. Among the geometric variables, baffle pitch—the axial spacing between consecutive baffles—plays a particularly influential role, as it governs the strength of the swirl flow, turbulence level, residence time, and hydraulic resistance within the exchanger [3,6,16].

In the present work, a computational fluid dynamics (CFD) approach was adopted to investigate the shell-side performance of a helical-baffle shell-and-tube heat exchanger with varying baffle pitches. The geometry was constructed using CATIA, and simulations were performed in ANSYS Fluent, including post-processing of thermal and flow parameters [4,10]. The numerical analysis examines the influence of baffle pitch variation (26–50 mm) on shell-side pressure drop, temperature reduction, and overall heat transfer rate under a range of mass flow conditions [2,9].

Recent developments in this area have introduced hybrid and variable-pitch helical designs that further expand the design space and the potential efficiency of such exchangers. A comprehensive review on helical baffle heat exchangers has outlined advancements in geometry optimization, hybrid baffle systems, and performance prediction frameworks [23]. Innovative configurations such as trefoil–zonal and other hybrid baffle arrangements have proved enhanced heat transfer performance while keeping acceptable pressure losses [24]. Numerical studies by Guo et al. [25] involving combined helical baffles and finned tubes have also reported higher overall efficiency compared with conventional segmental or continuous helical systems.

Moreover, the application of multi-objective optimization and computational intelligence algorithms has enabled precise determination of best design and operating variables [26]. Both experimental and CFD-based investigations on continuous helical baffles have shown that optimized spiral-flow designs yield superior heat recovery effectiveness in industrial systems [27].

Despite significant progress, most published studies have examined only fixed or limited baffle-pitch configurations, leaving uncertainty about how to find the best pitch that balances heat transfer enhancement and hydraulic performance. To bridge this research gap, the present study conducts a comprehensive CFD-based parametric analysis of baffle pitches ranging from 26–50 mm and shell-side mass flow rates. The results provide a quantitative understanding of how baffle spacing influences pressure drop, temperature drop, and heat transfer rate, thereby offering valuable design guidance and setting up practical benchmarks for perfecting shell-and-tube heat exchangers with helical baffles.

2. Problem identification

Conventional segmental baffle designs, though effective in directing shell-side flow to improve heat transfer, suffer from several inherent drawbacks. These include:

- Significant pressure drops resulting from abrupt directional changes in the fluid path.
- Flow-induced vibrations that can contribute to long-term structural fatigue.
- Formation of stagnant regions and non-uniform flow distribution within portions of the shell.
- Inefficient use of the total heat transfer surface area.

In contrast, helical baffle configurations have gained prominence as an improved alternative because they guide the fluid along a continuous spiral path, enabling smoother flow, lower pressure loss, and enhanced heat transfer performance. Nevertheless, the effectiveness of helical baffles is strongly governed by the baffle pitching the axial distance separating consecutive baffles [6,13]. Although many investigations have explored helical baffle designs, the best pitch that yields the highest heat transfer efficiency while keeping acceptable pressure characteristics for specific operating conditions stays inadequately defined [12,19].

So, this study emphasizes the necessity for a systematic CFD-based analysis aimed at:

- Quantitatively evaluating the influence of baffle pitch on the combined thermal and hydraulic performance of the heat exchanger.
- Finding a best pitch that achieves a balanced trade-off between pressure drop and heat transfer enhancement.
- Providing flow-field visualizations that clarify the internal flow structure, turbulence behavior, and temperature distribution within the shell region.

3. Aims of the work

The primary goal of this research is to analyze and improve the performance of a shell-and-tube heat exchanger fitted with helical baffles by perfecting the baffle pitch. To achieve this aim, the following specific aims were set up:

1. To develop a correct three-dimensional model of a shell-and-tube heat exchanger incorporating helical baffles using CATIA V5 design software.
2. To carry out CFD simulations of shell-side fluid flow and thermal transport in ANSYS Fluent 15.0, considering a range of baffle pitches and mass flow rates.
3. To quantitatively evaluate the influence of baffle pitch variation on major performance indicators, including:
   - Pressure drops (Pa)
   - Temperature difference(°C)
   - Heat transfer rate(W)
4. To examine internal flow phenomena and interpret shell-side fluid behavior through visualization tools such as streamline distributions, velocity vector fields, and temperature contour plots.
5. To decide the best baffle pitch provides the most favorable compromise between enhanced heat transfer capability and acceptable pressure drop.

4. Methodology

A systematic computational method was adopted to achieve best thermal performance of the shell-and-tube heat exchanger equipped with helical baffles. The procedure integrates 3D geometric modeling, CFD-based thermal–hydraulic analysis, and comprehensive post-processing evaluation. The methodological framework is outlined below.

4.1. Geometric modeling

- A three-dimensional model of the shell-and-tube heat exchanger with helical baffles was created using CATIA V5 software.
- The helical baffle pitch varied systematically at 26 mm, 30 mm, 34 mm, 38 mm, 42 mm, 46 mm, and 50 mm to study its influence on shell-side performance.
- The shell-and-tube dimensions were kept constants for all configurations to ensure that only the effect of baffle-pitch variation was analyzed.

4.2. Meshing

- The computational domain was discretized using a structured tetrahedral mesh with sufficient refinement near wall boundaries to capture velocity and thermal gradients accurately.
- Appropriate inflation layers were included to resolve boundary layer effects and keep grid independence.

4.3. Simulation setup in ANSYS fluent

- Solver Type: Pressure-based, steady-state solver.
- Turbulence Model: Realizable k–ε turbulence model with enhanced wall treatment for correct near-wall predictions.
- The working fluid was water, which was considered the shell-side medium.

Boundary Conditions:

- Shell-side mass-flow inlets were defined for flow rates ranging from 0.1571 to 0.6284 kg/s.
- Temperature boundary conditions were applied at both hot and cold inlets.
- The shell outlet was modeled with an outflow boundary condition to allow the pressure to adjust naturally.

4.4. Post-processing

- The simulation outputs were examined through contour plots of temperature, pressure, and velocity, enabling visualization of flow structure and temperature distribution.
- Streamline plots were employed to interpret fluid trajectories and find zones of recirculation or bypass flow.
- Quantitative performance data were obtained, including:
  - Pressure drops across the shell side (Pa).
  - Temperature difference between inlet and outlet(°C).
  - Heat transfer rate(W), computed from the energy balance relation.

4.5. Comparative analysis

Simulation data corresponding to various baffle pitches and mass flow rates were systematically tabulated and analyzed.

- A comparative assessment was performed to decide the configuration, yielding the best compromise between enhanced heat transfer and an acceptable pressure drop.
- The analysis was repeated at different mass flow rates: m1 = 0.1571Kg/s, m2 = 0.2356Kg/s, m3 =0.3142Kg/s, m4= 0.37704Kg/s, m5= 0.4713Kg/s, m6= 0.5499Kg/s and m7 = 0.6284Kg/s

5. Modeling procedure in CATIA for helical baffle shell-and-tube heat exchanger

The geometric modeling of the shell-and-tube heat exchanger was performed using the Part Design, Sketcher, Assembly Design, and Wireframe and Surface Design workbenches in CATIA V5.

Step 1: Define the Basic Dimensions and Layout

The key geometrical parameters for the heat exchanger model are summarized below:

- Material: Copper
- The internal tube diameter: 16mm
- Tube external diameter: 20mm
- Number of tubes: 02
- Tube effective length: 200mm
- Shell internal diameter: 50mm

This dimensional planning ensures accurate proportions and facilitates precise assembly.

Figures 1 and 2 illustrate the modeled shell-and-tube heat exchanger with the helical baffle configuration.

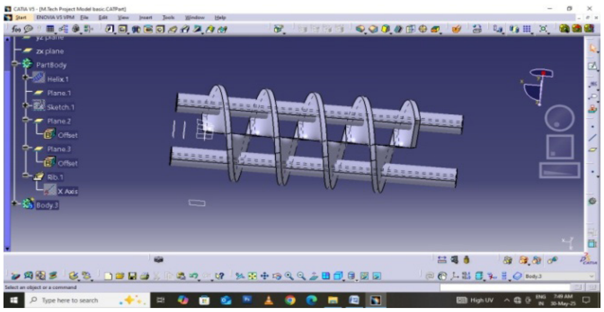

Figure 1: Helical structure of shell and tube heat exchanger

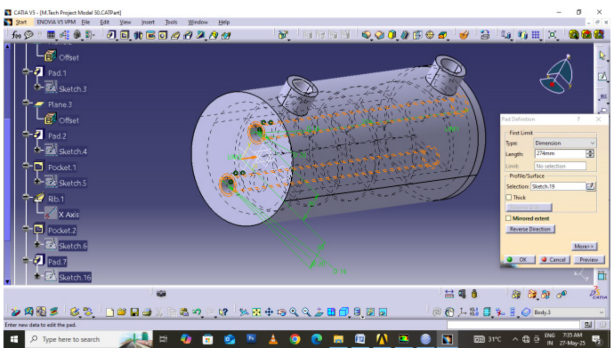

Figure 2: Shell and tube heat exchanger with helical baffle structure using Catia V5

A similar procedure was employed to generate a series of models with varying helical baffle pitches. Seven models (Models 1–7) were prepared with pitch values ranging from 26 mm to 50 mm, in 4-mm increments, being 50% to 100% of the shell diameter. This systematic variation allows for a comprehensive study of the effect of baffle pitch on heat exchanger performance.

6. Analysis procedure using ANSYS fluent 15.0

The computational investigation of the shell-and-tube heat exchanger was performed using ANSYS Fluent 15.0 to examine the influence of varying helical baffle pitches on shell-side pressure drop, temperature difference, and heat transfer rate. The analysis procedure is summarized as follows:

Step 1: Geometry Import and Fluid Domain Definition

- The 3D CATIA model of the heat exchanger was imported into ANSYS Workbench.
- Using Design Modeler, the fluid domain was extracted, the regions occupied by the shell-side and tube-side fluids (corresponding to Figures 3 and 4).

Step 2: Meshing

The fluid and solid domains were discretized using ANSYS Meshing Tool (Figure 5).

- A grid independence study was conducted to ensure mesh insensitivity of results, considering three mesh densities:
  - Coarse mesh: 0.45 million elements
  - Medium mesh: 0.78 million elements
  - Fine mesh: 1.12 million elements
- The shell-side heat transfer coefficient and pressure drop were checked for each mesh. Variations between medium and fine meshes were below 2% for heat transfer and 1.5% for pressure drop, confirming the balance between computational efficiency and accuracy.
- Fine tetrahedral elements with inflation layers were used near the walls to accurately resolve boundary layer effects.

Step 3: Boundary Identification

Boundaries for inlets, outlets, and walls were properly named in the meshing environment to ease correct solver setup.

Step 4: Solver Configuration in Fluent

The meshed domain was imported into ANSYS Fluent, where the following settings were applied (Figure 6):

- Solver Type: Pressure-based, steady-state
- Energy Equation: Enabled for temperature calculations
- Turbulence Model: Realizable k–ε with enhanced wall treatment for correct near-wall predictions
- Material Definitions:
  - Fluid: Water (from Fluent database)
  - Solid: Copper for tube and shell walls

Step 5: Boundary Conditions

- Inlets (Hot and Cold):
  - Modeled as velocity inlets
  - Velocity range: 0.5–2 m/s(corresponding to desired mass flow rates)
  - Temperature: Hot side = 90°C, Cold side = 15°C
- Outlets (Hot and Cold):
  - Treated as pressure outlets with 0 Pa gauge pressure
- Wall Conditions:
  - Tube and shell walls are defined as coupled walls to account for heat conduction through the solid domain

Step 6: Solution Controls and Initialization

- Standard solver controls were applied with refinements for enhanced accuracy:
  - Pressure-velocity coupling: Coupled
  - Discretization schemes: Second-order upwind for momentum, energy, and turbulence equations

Computational Fluid Dynamics is based on the following governing equations:

Continuity Equation:

$\nabla \cdot \upsilon = 0$

Where:

υ: velocity vector field

Momentum Equations:

$$\partial \frac{\partial \upsilon}{\partial t} + (\upsilon . \nabla)\upsilon = -\nabla p + \mu \nabla^2 \upsilon + F$$

Where:

ρ: fluid density, p: static pressure

μ: dynamic viscosity, F: body force (e.g., gravity)

Energy Equation (Heat Transfer):

$$\rho c_p \frac{\partial T}{\partial t} + \upsilon . \nabla T = \nabla . (k \nabla T) + \Phi$$

Where:

T: temperature, cp: specific heat

k: thermal conductivity, Φ: viscous dissipation term

This equation models temperature variation in both fluids and, if Conjugate Heat Transfer (CHT) is used, also in solids (e.g., tube walls and baffles).

Turbulence Modeling Equations

Two extra transport equations:

- Turbulent kinetic energy(k):
$$\frac{\partial \rho k}{\partial t} + \nabla \cdot (\rho v k) = \nabla \cdot (\alpha_k \mu_{eff} \nabla k) + G_k - \rho \epsilon$$
- Dissipation rate(ε):
$$\frac{\partial \rho \epsilon}{\partial t} + \nabla \cdot (\rho v \epsilon) = \nabla \cdot (\alpha_\epsilon \mu_{eff} \nabla \epsilon) + C_{1\epsilon} \frac{\epsilon}{k} G_k - C_{2\epsilon} \rho \frac{\epsilon^2}{k}$$

Symbol	Meaning
ρ	Fluid density (kg/m³)
k	Turbulent kinetic energy (m²/s²)
ϵ	Turbulent dissipation rate (m²/s³)
υ	Velocity vector (m/s)
G_k	Production of turbulent kinetic energy due to velocity gradients
μ_{eff}	Effective viscosity =μ+
μ	Molecular (laminar) viscosity (Pa·s)
μ_t	Turbulent (eddy) viscosity (Pa·s), modeled separately (see below)
α_k	Inverse effective Prandtl number for k
α_ϵ	Inverse effective Prandtl number for ε
$C_{1\epsilon}$	Empirical constant (≈ 1.44)
$C_{2\epsilon}$	Empirical constant (≈ 1.92)

Step 7: Simulation Execution

- CFD simulations were carried out until the residuals of the continuity, momentum, and energy equations fell below 10^{-5}, ensuring numerical convergence.
- Convergence was further confirmed by tracking critical performance parameters, such as shell-side pressure drop and outlet temperature, which showed minimal variation (<0.5%) over later iterations.
- These checks guaranteed that the computed solutions were stable, correct, and fully converged.

Step 8: Post-Processing

Fluid flow and heat-transfer analyses were performed in ANSYS Fluent using its post-processing tools to visualize flow patterns and quantify performance metrics.

a) Contour Analysis

- Pressure contours: Examined to decide shell-side pressure variations.
- Temperature contours: Used to assess thermal distribution across the shell and tube bundle.
- Velocity size contours: Highlighted regions of fluid acceleration and deceleration within the shell.

b) Vector Plots

- Velocity vectors were generated to reveal flow directions, swirling motion, and recirculation zones induced by the helical baffle arrangement.

c) Streamline Visualization

- Streamlines for both hot and cold streams were plotted to evaluate flow mixing, flow trajectory, and the impact of the helical baffle geometry on the fluid path length.

d) Quantitative Data Extraction

- Pressure drop was calculated as the shell-side inlet and outlet pressures for each baffle pitch.
- Temperature drop: Determined as the difference between cold stream inlet and outlet temperatures.
- Heat transfer rate: Determined using energy equation:
  Q = m. Cp. ΔT

Where: m = Mass flow rate, C_p = Specific heat of water, ΔT = Temperature difference

Figures 3–6 illustrate the analysis performed in ANSYS Fluent.

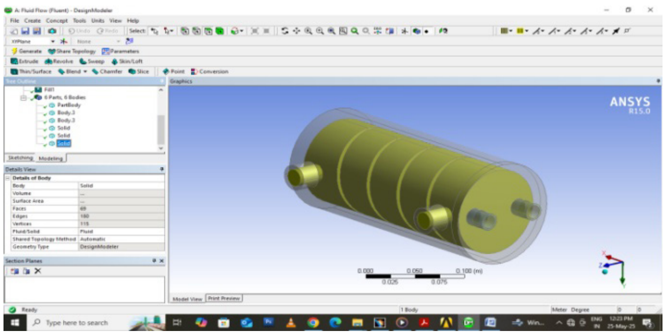

Figure 3. Fluid volume of shell side

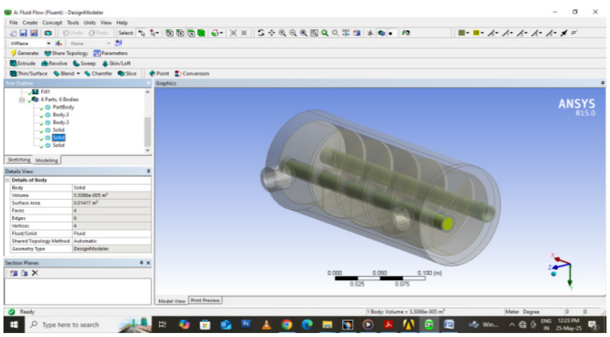

Figure 4. Fluid domains created at tube side

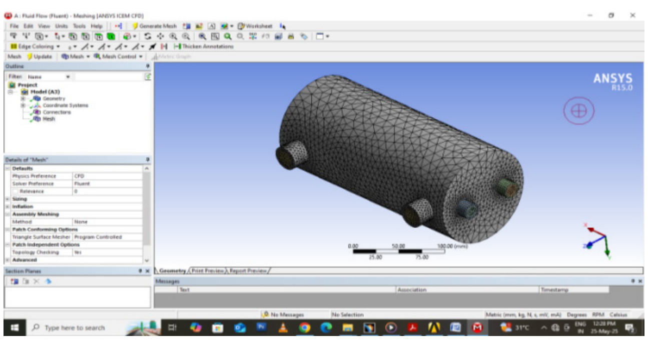

Figure 5. Meshing of created model in ANSYS Fluent

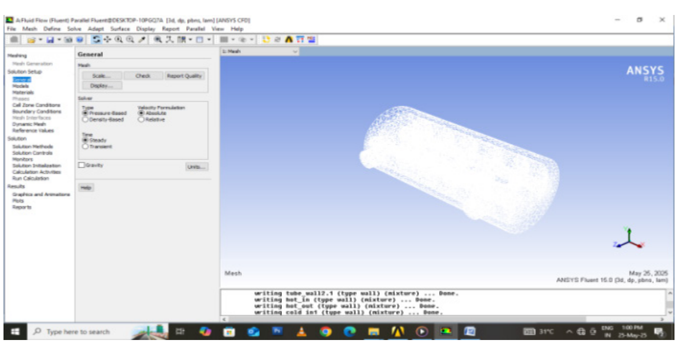

Figure 6: Setting steady state condition in setup of ANSYS Fluent

The pressure, velocity, and temperature data were recorded, and streamlines and velocity vectors were generated; these were analyzed in the following section.

7. Results and discussions

7.1. Simulation results of a model

7.1.1. Pressure distribution: flow resistance and losses

The pressure contours shown in Figure 7 illustrate a gradual transition from high-pressure regions (red/yellow) to low-pressure areas (blue/green) along the shell-side flow path. This pattern reflects the typical pressure losses due to viscous drag along the tube and shell walls, with minor contributions from geometric features such as bends, contractions, and expansions [1, 4, 7]. Elevated pressures near the inlet show localized resistance or backpressure before the fluid accelerates. Such losses are common in heat exchangers and represent the energy needed to overcome flow resistance [6, 17].

The pressure streamlines in Figure 16 further support this observation, showing a consistent pressure gradient from the shell inlet to the outlet. Pressure is highest at the entry region, where the fluid affects the first baffle, and gradually decreases along the flow path. The smooth reduction in pressure reflects the lower flow resistance of the helical-baffle design compared with conventional segmental baffles. This balanced pressure distribution shows the best compromise between turbulence enhancement for heat transfer and manageable hydraulic losses. Consequently, the analysis confirms that the proposed baffle geometry improves thermal–hydraulic performance, enabling effective fluid mixing and efficient heat exchange.

7.1.2. Velocity distribution: flow acceleration and streamline behavior

The velocity contours in Figure 8 reveal variations in shell-side fluid velocity, with high-velocity regions in red and yellow and velocity regions in blue and green. Acceleration is seen in constricted areas due to reduced cross-sectional flow, producing a Venturi-like effect that enhances local momentum and convective heat transfer [2, 3, 6]. According to Bernoulli's principle, velocity increases correspond with local pressure reductions, proving the expected pressure–velocity relationship [11, 18]. Regions transitioning from blue to red may also show changes in flow regime, from laminar to turbulent [13, 16].

Figures 12–14 present velocity vector distributions along the shell side, covering the inlet, flow development, and outlet regions.

- In the inlet region (Figure 12), velocity vectors show that the incoming fluid is sharply redirected by the first helical baffle, creating high-velocity jets near the baffle openings and recirculation zones in wake regions. This promotes fluid mixing and starts secondary flows, which disrupt boundary layers and enhance shell-side heat transfer.
- Mid-section (Figure 13): Vectors show strong crossflow motion across the tube bundle. The helical baffle arrangement forces the fluid into a spiral path, encouraging continuous redirection and uniform flow distribution across

successive tubes, and reducing dead zones commonly saw in conventional designs.

- In the outlet region (Figure 14), velocity vectors realign to a more uniform pattern, minimizing maldistribution and reducing hydraulic losses.

Overall, the velocity vector plots prove that the helical baffles induce a continuous swirling motion, achieving two primary effects: (i) enhanced turbulence and fluid mixing, leading to higher heat transfer coefficients, and (ii) a stable velocity field at the outlet, reducing pressure losses.

Additionally, the velocity streamlines in Figure 15 confirm improved flow uniformity and reduced bypassing, proving the effectiveness of the helical baffle design in enhancing thermo-hydraulic performance. The observed improvements are attributed to reduced dead zones and increased turbulence intensity along the helical flow path.

7.1.3. Temperature distribution in the cold tube: heat absorption

Figure 9 presents the temperature distribution across the shell and tube sides of the heat exchanger, confirming effective heat transfer between the shell-side and tube-side fluids [3, 6]. Due to the wide range of temperatures depicted, local variations are not at once clear. To offer a clearer view, post-processed contour plots were generated for specific temperature ranges:

- Figure 10: Focused on lower temperatures to examine the cold fluid stream.
- Figure 11: Covered a broader temperature range to capture shell-side behavior [4, 5].

In Figure 10, the tube-side temperature is predominantly depicted in blue to green, showing the cold fluid entering the tubes and gradually warming along its path. This pattern proves effective heat absorption by the tube-side fluid, showing efficient convective heat transfer [7, 10]. A steady temperature gradient along the flow path reflects moderate convective performance, which can be further enhanced through increased turbulence or extended surface area designs such as fins [12, 15].

7.1.4. Temperature distribution in the shell: heat release

Figure 11 shows the shell-side temperature contours, with dominant red/yellow regions gradually transitioning to orange/green toward the outlet. This distribution reflects progressive heat transfer from the hot fluid to the colder tube-side stream [4, 6]. The gradual color change highlights the effectiveness of energy exchange, eased by adequate fluid mixing and sufficient residence time within the shell [5, 7].

The color gradients also reveal the formation of the thermal boundary layer, with higher heat transfer shown by a more pronounced decrease in temperature along the flow direction [8, 13]. The use of helical baffles promotes turbulence and swirling, further enhancing convective heat transfer and ensuring a uniform temperature profile [10, 12].

Table 1 provides a detailed comparison of predicted and computed (CFD-obtained) values for pressure, velocity, and temperature, thereby evaluating simulation performance.

Table 1. Comparative assessment of predicted and simulated results

Aspect	Before (Assumed)	After (Observed)	Explanation
Pressure	More abrupt drop	More uniform gradient	Reduced friction / improved flow path
Velocity	Uneven acceleration	Smoother high-velocity zones	Better flow channeling, turbulence tuning
Cold Temp	Sudden jump or limited change	Smooth increase, higher exit temp	More effective heat uptake, possibly longer tube
Hot Temp	Persistent red/yellow	Gradual fades to orange	More heat released to cold stream, higher effectiveness

A comparative assessment of the system states before and after simulation highlights the following trends:

- Pressure and Velocity: The velocity field exhibits more uniform and streamlined flow patterns, accompanied by a moderate reduction in pressure drop. These improvements show enhanced flow dynamics, likely resulting from optimized geometry and reduced flow resistance.
- Cold Tube and Hot Shell Temperature: The temperature distribution shows a broader, more continuous gradient across both the shell and tube sides, showing improved heat transfer performance. This enhancement is attributed to better flow alignment and increased turbulence, which promotes more effective convective heat exchange.

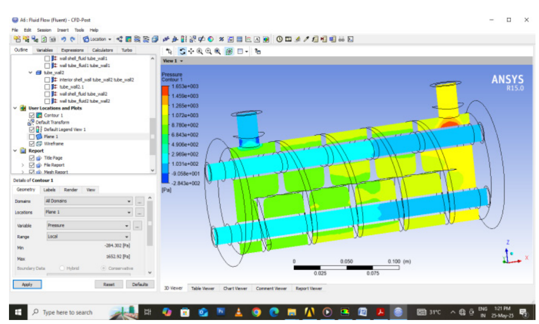

Figure 7. Pressure counter in post CFD- ANSYS Fluent

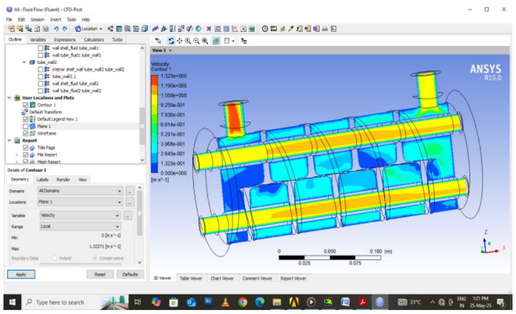

Figure 8. Velocity counter in post CFD- ANSYS Fluent

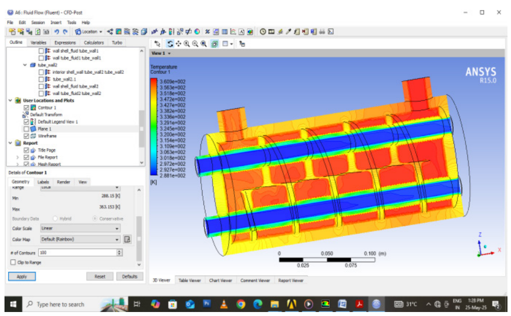

Figure 9. Temperature counter in post CFD- ANSYS Fluent

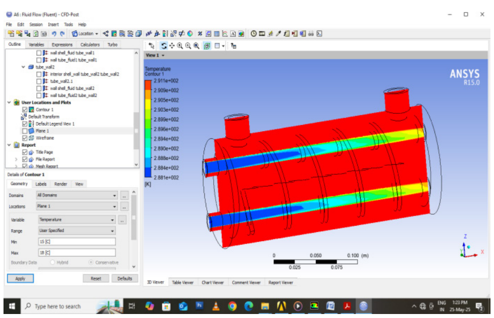

Figure 10. Tube side temperature counter in post CFD- ANSYS Fluent

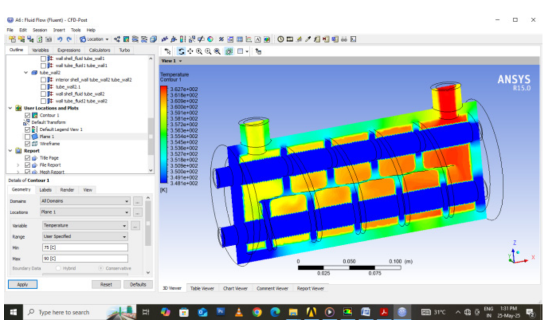

Figure 11. Shell side temperature counter in post CFD-ANSYS Fluent

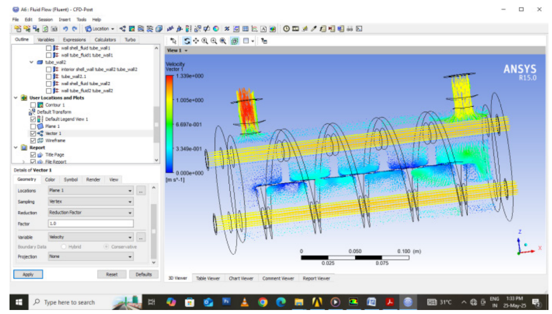

Figure 12. Velocity vector plot in post CFD ANSYS Fluent

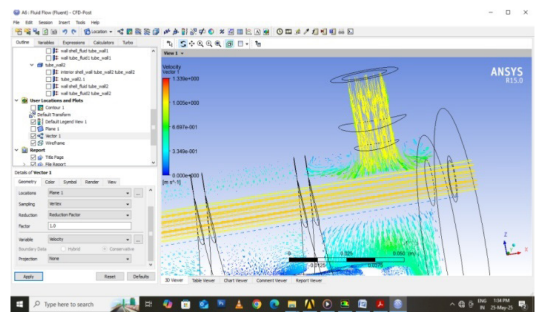

Figure 13. Shell side inlet velocity vector in post CFD ANSYS Fluent

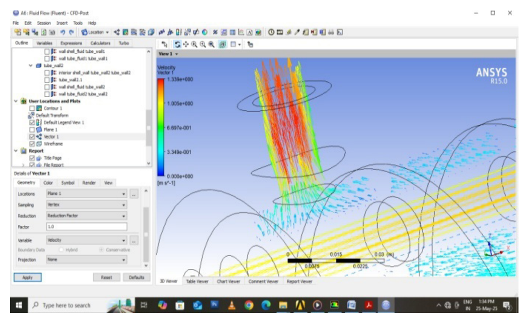

Figure 14. Shell side outlet velocity vector in post CFD ANSYS Fluent

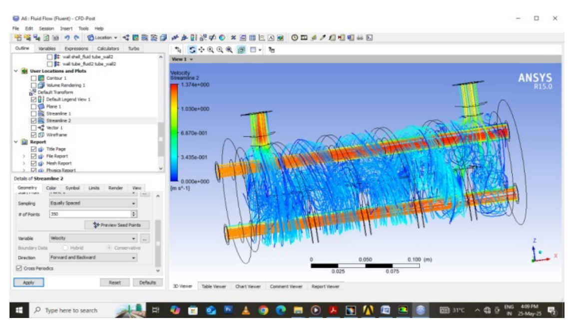

Figure 15. Velocity Streamlines obtained in post CFD-ANSYS Fluent

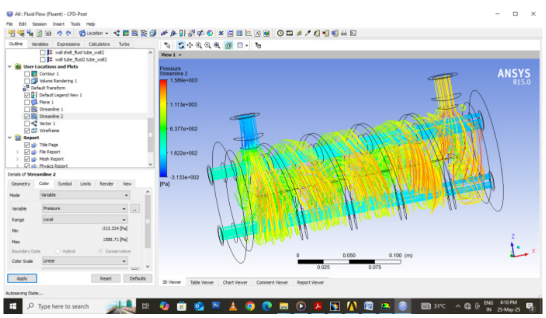

Figure 16. Streamlines of pressure through post CFD ANSYS Fluent

7.2. Comparative analysis of simulation results

7.2.1. Shell-side pressure drop in helical baffle heat exchangers

a) Simulation Results and Flow Characteristics: The shell-side pressure drop was evaluated using ANSYS Fluent for helical-baffle pitches ranging from 26 mm to 50 mm and shell-side mass flow rates between 0.1571 and 0.6284 kg/s, as shown in Figure 17. The simulations show that pressure drop generally decreases as the baffle pitch increases from lower to moderate values and tends to stabilize or slightly rise at the largest pitches, particularly at lower flow rates [3, 6].

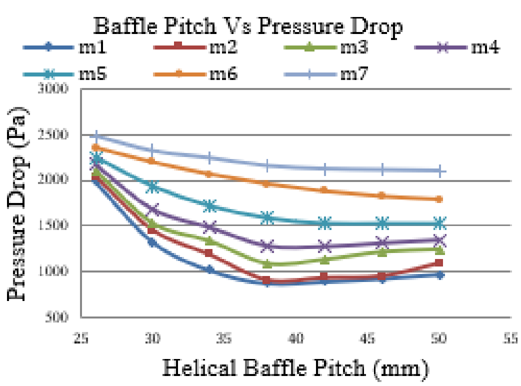

Figure 17. Variation of Pressure drop at different helical baffle pitch with different shell side mass flow rate

As the fluid navigates through the helical baffles around the tube bundle, friction and flow redirection contribute to pressure losses [4, 11]. Helical baffles guide the fluid along a spiral path, reducing dead zones and promoting swirling motion, which improves overall fluid distribution [6, 13]. Smaller pitches increase turbulence intensity and flow path length, resulting in higher resistance [3, 16]. Compared with conventional segmental baffles, the helical arrangement reduces flow impingement, thereby lowering peak pressure losses.

Key Observations:

- The Pressure drop decreases with increasing baffle pitch across all flow rates.
- At 0.6284 kg/s, the pressure drops decrease from 2475 Pa (26 mm pitch) to 2105 Pa (50 mm pitch).
- A lower pitch (e.g., 26 mm) introduces more obstructions, increasing friction and the flow path length.
- A higher pitch (e.g., 50 mm) allows more axial flow, reducing directional changes and friction.
- The Maximum pressure drops at a 26 mm pitch ranges from 1985 to 2475 Pa.
- At 38 mm, the pressure drops range from 873 to 2156 Pa, showing smoother flow.
- At 50 mm, pressure drop decreases further to 972.4–2105 Pa, showing reduced turbulence.
- Flow visualization confirms that tighter pitches generate high turbulence zones and backflow, contributing to energy losses.

Overall, the trend aligns with expectations: smaller pitches result in higher resistance, while larger pitches reduce friction but may lower turbulence levels.

b) Manufacturing and Design Considerations: Tighter baffle spacing requires more baffles per unit length, increasing material usage and fabrication complexity. Wider baffle pitches simplify manufacturing and reduce the number of baffles, but they may compromise heat transfer efficiency. Larger pitch values ease cleaning and maintenance, reducing operational downtime and costs. Excessively tight spacing can create stagnant zones, raising the risk of vibration and fouling. A pitch of 38 mm provides a balanced design, supporting structural integrity while keeping pressure drop within acceptable limits.

c) Influence on Flow Patterns:

Baffle pitch directly affects the spiral flow path:

- Smaller pitch → tighter spiral, increased velocity fluctuations, higher shear stresses, and greater pressure drop.
- Larger pitch → gentler spiral, smoother flow, lower turbulence, and reduced friction.

- High-pressure losses at very low pitches are caused by secondary flows and eddies, which can induce vibration or fouling during prolonged operation.
- Streamline plots reveal intense vortices and secondary flows at low pitch, increasing resistance while enhancing convective heat transfer.
- Beyond a certain turbulence level, added pumping costs may outweigh thermal benefits.
- Larger pitches reduce swirling and partial bypass, lowering friction, but causing underutilization of the heat-transfer surface.

A medium pitch (38 mm) achieves the best balance, generating sufficient swirl for effective heat transfer while minimizing back pressure).

Practical Implications:

- High pressure drops increase pumping power requirements, affecting energy consumption and operational costs.
- Continuous-operation systems receive help from designs that minimize shell-side ΔP.
- Selecting a 38-mm pitch reduces pressure drop by 30–40% compared with tighter designs, without significantly affecting heat transfer performance.

7.2.2. Shell-side temperature drop in helical baffle heat exchangers

a) Simulation Results and Flow Characteristics:

The shell-side temperature drop was analyzed using ANSYS Fluent for helical baffle pitches ranging from 26 mm to 50 mm and mass flow rates ranging from 0.1571 to 0.6284 kg/s, as shown in Figure 18. The results show a nonlinear trend: the temperature drop initially increases with baffle pitch, reaches a maximum at moderate spacing, and decreases at larger pitches. This behavior is more pronounced at lower mass flow rates [2, 6].

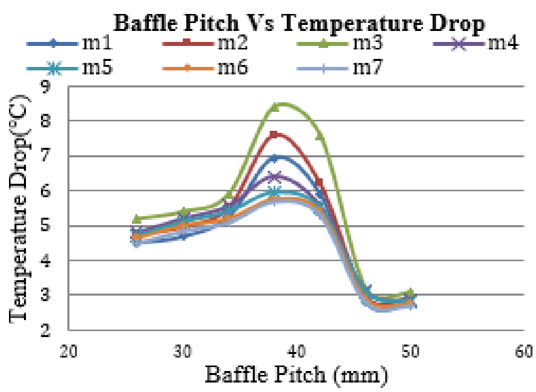

Figure 18. Variation of temperature drop at different helical baffle pitches with different shell side mass flow rate

Key Observations:

- The maximum temperature drop of 8.4°C occurs at a baffle pitch of 38 mm and a mass flow rate of 0.3142 kg/s, proving the best balance between turbulence and flow stability.
- Smaller pitches (26 mm) show limited temperature drops (4.5–5.2°C) because excessive pressure losses reduce fluid residence time, and thus lower heat-transfer efficiency.
- Moderate pitches (34–38 mm) show superior thermal performance owing to:
  - Enhanced crossflow across the shell,
  - Uniform fluid distribution, and
  - Controlled turbulence intensity, which ensures effective energy exchange.
- Larger pitches (46–50 mm) result in reduced temperature drops (2.7–3.2°C) due to weaker mixing, flow channeling, and a predominance of axial flow, all of which diminish heat transfer surface use.

Interpretation:

- Very small pitches, while increasing turbulence, can lead to high flow resistance, creating recirculation and blockage zones that reduce effective heat transfer.
- Excessively large pitches produce insufficient turbulence, resulting in poor mixing and lower thermal gradients.
- A baffle pitch of 38 mm provides the optimal compromise between turbulence and flow stability, achieving efficient shell-side heat transfer and hydraulic performance.

b) Manufacturing and Design Considerations:

- Narrow baffles (26 mm) present maintenance and cleaning challenges, particularly in fouling-prone systems.
- Wider baffle spacing simplifies fabrication and maintenance but compromises thermal performance.
- Baffle pitches in the range of 34–38 mm offers high thermal absorption while keeping practical manufacturability and operational ease.
- The 38 mm pitch promotes faster thermal equilibration, improving overall system efficiency and ensuring stable long-term performance.

c) Influence on Flow Patterns:

- At the best 38 mm pitch, shell-side flow shows well-developed, swirl that enhances boundary-layer disruption and fluid penetration toward the tube surfaces, resulting in a more uniform temperature distribution and improved heat transfer.
- At 26 mm, excessive flow resistance creates stagnation and recirculation zones, reducing effective temperature gradients.
- At 50 mm, laminar-like flow patterns dominate due to stable thermal boundary layers, leading to weaker turbulence and reduced heat transfer.
- Optimal helical whirling along the length of the tube bundle promotes uniform heat absorption, while tight pitches cause chaotic temperature variations, and wide pitches allow flow to bypass active heat-transfer zones.

d) Practical Implications:

- During operation, the ideal baffle configuration maximizes temperature drop while minimizing energy penalties due to pressure losses.
- Although increased turbulence generally improves heat transfer, it also increases pumping power.

The observed "sweet spot" at 38 mm balances thermal performance and hydraulic efficiency, confirming its choice for enhancing shell-and-tube heat exchanger performance.

7.2.3. Shell-side heat transfer rate in helical baffle heat exchangers

a) Simulation Results and Flow Characteristics

The shell-side heat transfer rate (Q) was examined using ANSYS Fluent for helical baffle pitches ranging from 26 mm to 50 mm and mass flow rates between 0.1571 and 0.6284 kg/s, as summarized in Figure 19. The analysis reveals a non-linear relationship: Q increases with baffle pitch up to a best value near 38 mm and declines beyond this pitch for all flow rates [3, 6].

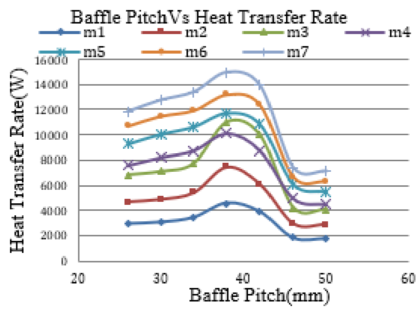

Figure 19: Variation of heat transfer rate at different helical baffle pitches with different shell side mass flow rate

Key Observations:

- The maximum heat transfer rate of 14,972 W occurs at a baffle pitch of 38 mm and a mass flow rate of 0.6284 kg/s, reflecting the combined effects of enhanced turbulence, efficient fluid mixing, and adequate residence time.
- Smaller pitches (26 mm) create excessive flow obstruction and a high pressure drop, thereby limiting effective surface use and reducing overall heat transfer.
- Larger pitches (46–50 mm) allow flow bypass and axial channeling, which decrease the interaction between the shell-side fluid and the tube bundle.
- Overall, the heat transfer rate shows a non-linear dependence on baffle pitch, the 38 mm pitch achieves over 25% higher Q than the 26 mm and 50 mm configurations.
- Across all baffle pitches, Q increases with mass flow rate despite a reduction in temperature difference (ΔT) at higher flow rates, indicating that convective enhancement dominates the heat transfer behavior within the tested range.

Explanation:

- The observed trends result from the interplay of flow turbulence, residence time, and pressure drop. At 38 mm, turbulence is sufficient to enhance mixing without excessive hydraulic losses, yielding uniform temperature distribution and higher convective heat transfer.
- At 26 mm, high resistance limits effective mass flow and area use, while at 46–50 mm, weak turbulence and bypass flow reduce fluid–tube interactions.
- Consequently, the 38-mm pitch provides the best flow regime combining moderate turbulence, uniform distribution, and minimal obstruction, achieving the best thermo-hydraulic balance.

b) Manufacturing and Design Considerations:

- The number of baffles affects both performance and fabrication cost. Tight baffle spacing increases material usage, weight, and cleaning complexity, while looser spacing reduces costs but can compromise heat transfer.
- The 38 mm pitch offers the best compromise, keeping a moderate baffle count to reduce fabrication and operational challenges while sustaining high heat transfer and low-pressure losses.
- This configuration ensures energy-efficient operation and reliable system performance, making it suitable for industrial applications where both performance and economy are important.

c) Influence on Flow Patterns:

- CFD visualizations show that, at the shell-side flow follows a spiraling and sweeping path, effectively covering tube surfaces and minimizing stagnant regions.
- Velocity vector fields show high-shear zones around the tubes, enhancing convective heat transfer through increased momentum exchange.

d) Practical Implications:

- Although increased heat transfer typically goes with higher frictional losses, the 38-mm pitch achieves a balanced Performance Evaluation Criterion (PEC) by maximizing Q while claiming a moderate pressure drop.
- The correlation between enhanced turbulence and improved heat transfer shows that forced convection is dominant in this configuration.
- Therefore, a 38 mm baffle pitch is an efficient thermo-hydraulic design, offering robust performance with balanced energy consumption for industrial-scale heat exchangers.

7.3. Summary of thermal–hydraulic performance

To correctly evaluate the combined thermal and hydraulic behavior of the shell-and-tube heat exchanger at different baffle pitches, a new performance index was used:

Performance Index = $Q/\Delta P$ (W/Pa)

This index effectively is the heat transfer gained per unit of required pumping power, making it a reliable criterion for finding the best operating conditions. Higher $Q/\Delta P$ values show superior thermal-hydraulic efficiency, which is highly desirable in industrial heat exchangers.

Table 2 presents the key thermal–hydraulic performance metrics: temperature drop and heat transfer rate per unit pressure drop for different helical baffle pitches and shell-side mass flow rates. The analysis shows the following trends:

Lower baffle pitches (26mm to 30mm) promote strong shell-side turbulence due to frequent flow interruptions. This enhances heat transfer; however, the benefit is offset by a high pressure drop, which significantly reduces the Q/ΔP ratio.

Moderate (34mm to 38mm) pitches create a best balance between turbulence intensity and flow resistance. In particular, the 38 mm pitch shows the highest performance (10.12 W/Pa) among all cases.

Higher pitches (42mm to 50mm) reduce the number of flow redirections, resulting in a lower pressure drop but also in weaker turbulence. Although the pressure drop is low, the corresponding decline in heat transfer causes a sharp reduction in thermal-hydraulic efficiency, especially beyond 46 mm.

Key Finding:

- Across all pitch groups, the 38 mm baffle pitch (at 0.3142 kg/s mass flow rate) provides the maximum thermal-hydraulic performance with a Q/ΔP value of 10.12 W/Pa.
- This shows that the 38 mm pitch provides the best trade-off between heat transfer enhancement and pressure drop, making it the most energy-efficient design for practical industrial applications.

Table 2. Performance metrics for different baffle pitches

Baffle Pitch (mm)	Mass Flow Rate (kg/s)	Temperature Drop ΔT (°C)	Heat Transfer Rate Per Unit Pressure Drop Q/ΔP (W/Pa)
26	0.6284	4.5	4.78
30	0.6284	4.85	5.50
34	0.4713	5.4	6.21
38	0.3142	8.4	10.12
42	0.3142	7.6	8.80
46	0.4713	3.1	4.01
50	0.4713	2.8	3.63

7.4. Comparison with recent studies

Recent research on helical baffle heat exchangers has focused on improving thermal–hydraulic performance. For instance, Guo et al. [25] reported that continuous helical baffles reduce pressure drop by 20–30% compared to conventional segmental baffles while enhancing heat transfer efficiency. This observation aligns with the present study, which finds that an intermediate baffle pitch of 38 mm offers a best compromise between thermal enhancement and pressure penalty. Similarly, Zhang et al. [26] proved that carefully perfected helical arrangements yield higher temperature drops with moderate pressure losses, supporting the current finding that the 38 mm pitch achieves an 8.4°C temperature drop under acceptable pressure conditions. Hybrid baffle designs discussed by Chen et al. [24] also highlight the necessity of balancing heat transfer improvement with pumping costs, which reinforces the identification of 38 mm as a best configuration in this study.

The distinguishing feature of the present work is the systematic, quantitative evaluation of performance across a wide range of baffle pitches (26–50 mm) using direct engineering metrics, including pressure drop (873–2156 Pa), heat transfer rate (14.9 kW), and temperature drop (8.4°C). Unlike earlier studies that reported qualitative trends, this investigation provides clear, actionable data suitable for practical industrial heat exchanger design.

8. Conclusion

- Baffle Pitch Significance: The baffle pitch is a key factor influencing both the thermal and hydraulic behavior of shell-and-tube heat exchangers with helical baffles.
- Tight Pitches (e.g., 26 mm):
  - Lead to higher pressure drops due to increased flow obstruction and turbulence.
  - Moderate temperature drops and reduced heat transfer performance are seen when fluid flow is restricted.
  - At 26 mm, the pressure drops increases by ap proximately 35% compared to that at 50 mm, while the heat transfer improves by around 20%.
- Large Pitches (46–50 mm):
  - Reduce pressure drop but cause flow bypassing, underutilizing the heat transfer surface and lowering thermal efficiency.
  - At 50 mm, the pressure drop is roughly 40% lower than at 26 mm, while the heat transfer is reduced by 25%.
- Optimal Pitch (38 mm):
  - It is the highest heat transfer rate of 14,972 W, which is 1.27 and 2.11 times the heat transfer rates at the tight pitch (26 mm) and the large pitch (50 mm), respectively.
  - Shows a temperature drop of 8.4°C, being 1.6 times higher than that of temperature drop at the tight pitch (26 mm) and 2.7 times higher than that of temperature drop at the large pitch (50 mm)
  - Maintains a moderate, energy-efficient pressure drop (873–2156 Pa) across the range of mass flow rates.
  - Flow visualization confirms the formation of stable, swirling patterns that maximize surface contact and reduce dead zones and enhance

convective heat transfer.
- Based on the thermal–hydraulic performance index (Q/ΔP), the 38 mm pitch provides an efficiency of 10.12 W/Pa, which is 2.12 times higher than at the tight pitch (26mm) and 2.79 times higher than at the large pitch (50mm). This confirms that the 38 mm pitch provides the best balance between heat transfer enhancement and hydraulic losses.

- Practical implications
  - The findings offer practical guidance for industries such as petrochemicals, power generation, HVAC (Heating, Ventilation and Air Conditioning), and refrigeration.

Author contributions

Dr. G. Maruthi Prasad Yadav: Conceptualization, method, software, investigation, formal analysis, visualization, validation, writing – original draft preparation. Mr. G. Md. Javeed Basha: Data curation, software support, investigation, validation, writing – review and editing. Dr. B. OmPrakash: Supervision, method, validation, technical review, writing – review and editing. Mr. E. Madan Manohar: Formal analysis, technical review, validation, writing – review and editing. All authors have read and approved the final version of the manuscript and agree to be accountable for all aspects of the work.

Declaration of interests

The authors declare that they have no known competing financial interests or personal relationships that could have appeared to influence the work reported in this paper.

Data availability

The data supporting the findings of this study are available from the corresponding author upon reasonable request. The computational models and simulation data generated during the current study are not publicly available but can be provided for academic and research purposes upon reasonable request.

Declaration of generative AI and AI-assisted technologies in the writing process

During the preparation of this manuscript, the authors used generative AI-assisted tools solely to improve the English language, grammar, readability, and overall presentation of the manuscript. These tools were not used to generate scientific ideas, conduct analyses, interpret results, prepare figures, or formulate the conclusions of the study. All scientific content, methodology, analyses, interpretations, and conclusions were developed, verified, and approved by the authors, who take full responsibility for the content of this publication.

References

[1] Zhang, M., Meng, F., & Geng, Z, "CFD simulation on shell-and-tube heat exchangers with small-angle helical baffles", Frontiers in Chemical Science and Engineering, 9(2),183–193, 2015, DOI: 10.1007/s11705-015-1510-x.

[2] De, D., K, T., & Bandyopadhyay, S, "Helical baffle design in shell and tube type heat exchanger with CFD analysis", International Journal of Heat and Technology, 35(2),567–576, 2021, DOI: 10.18280/ijht.350221

[3] Magalhães, M.L., Pereira, A.S., & Cartaxo, S.J.M, "Development of a transient model for evaluation of shell and tube heat exchanger with helical baffles applied for SiO2 nanofluid", Journal of Advanced Thermal Science Research, 5(2),179–188, 2018, DOI: 10.15377/2409-5826.2018.05.2

[4] Malviya, R.K, "CFD simulation of helical shell and tube heat exchanger using optimization techniques", Journal of Engineering Research, 11(1B),1–12, 2021, DOI: 10.36909/jer.11985

[5] Hasu, B.S., & Satynarayana Rao, G.V, "Design and analysis of a heat exchanger with helical baffles by using CFD", International Journal of Engineering Trends and Technology, 48(7),350–353, 2017, DOI: 10.14445/22315381/IJETT-V48P261.

[6] Gugulothu, R., & Sanke, N, (2022), "Effect of Helical Baffles and Water-Based Al_2O_3, CuO, and SiO_2 Nanoparticles in the Enhancement of Thermal Performance for Shell and Tube Heat Exchanger", Heat Transfer, 51(5),3768–3793, 2022, DOI: 10.1002/htj.22056.

[7] Yang, J. F., Zeng, M., & Wang, Q. W, "Investigation on Combined Multiple Shell-Pass Shell and Tube Heat Exchanger with Continuous Helical Baffles", Energy,115, 1572–1579, 2016, DOI: 10.1016/j.energy. 2016. 09.080

[8] Naqvi, S. M. A., & Wang, Q, "Numerical Comparison of Thermo-hydraulic Performance and Fluid-Induced Vibrations for STHXs with Segmental, Helical, and Novel Clamping Antivibration Baffles", Energies, 12(3),540, 2019, DOI: 10.3390/en12030540.

[9] Magalhães, M. L., Pereira, A. S., & Cartaxo, S. J. M, 2018, "Development of a Transient Model for Evaluation of Shell and Tube Heat Exchanger with Helical Baffles Applied for SiO_2 Nanofluid", Journal of Advanced Thermal Science Research, 5(2),179–188, 2018, DOI: 10.15377/2409-5826.2018.05.2.

[10] Bozorgan, N., et al, "Design and Thermal-Hydraulic Optimization of a Shell and Tube Heat Exchanger using Bees Algorithm", Thermal Science, 26(1B),693–703, 2021, DOI: 10.2298/TSCI200408240B.

[11] Perumal, S., et al., "Effects of Nanofluids on Heat Transfer Characteristics in Shell and Tube Heat Exchanger", Thermal Science, 26(2A),835–841, 2021, DOI: 10.2298/TSCI200408240B

[12] Yang, J. F., Zeng, M., & Wang, Q. W, "Effects of Sealing Strips on Shell-Side Flow and Heat Transfer Performance of a Heat Exchanger with Helical Baffles", Applied Thermal Engineering, 64(1),117–128, 2014, DOI: 0.1016/j.applthermaleng. 2013. 11.064.

[13] Salahuddin, U., Bilal, M., & Ejaz, H, "A Review of the Advancements Made in Helical Baffles Used in Shell and Tube Heat Exchangers", International Communications in Heat and Mass Transfer, 67, 104–08, 2015, DOI: 10.1016/j. icheatmasstransfer. 2015.07.005.

[14] Zhang, J., Li, B., Huang, W.-T., Lei, Y. G., He, Y.-L., & Tao, W., "Experimental Performance Comparison of Shell-Side Heat Transfer for Shell-and-Tube Heat Exchangers with Middle-Overlapped Helical Baffles and Segmental Baffles", Chemical Engineering Science, 64(7), 1643–1653, 2009, DOI: 10.1016/j.ces.2008.12.018

[15] Yu, C., Ren, Z., & Zeng, M, "Numerical investigation of shell-side performance for shell and tube heat exchangers with two different clamping type anti-vibration baffles", Applied Thermal Engineering, 133, 125–136, 2018, DOI: 10.1016/j. applthermaleng.2018.01.029.

[16] Ji, J., Li, F., Shi, B., & Chen, Q, "Analysis of the effect of baffles on vibration and heat transfer characteristics of elastic tube bundles", International Communications in Heat and Mass Transfer, 136, 106206, 2022, DOI: 10.1016/j.icheatmasstransfer. 2022. 106206.

[17] Wen, J., Gu, X., Wang, M., Wang, S., & Tu, J, "Numerical investigation on the multi-objective optimization of a shell-and-tube heat exchanger with helical baffles", International Communications in Heat and Mass Transfer, 89, 91–97, 2017.

[18] Zhang, J., Li, B., Huang, W.-T., Lei, Y. G., He, Y.-L., & Tao, W, "Experimental performance comparison of shell-side heat transfer for shell-and-tube heat exchangers with middle-overlapped helical baffles and segmental baffles", Chemical Engineering Science, 64(7), 1643–1653, 2009, DOI: 10.1016/j. ces.2008. 12.018

[19] Yang, J.-F., Zeng, M., & Wang, Q.W., "Effects of sealing strips on shell-side flow and heat transfer performance of a heat exchanger with helical baffles", Applied Thermal Engineering, 64(1),117–128, 2014, DOI: 10.1016/j. applthermaleng. 2013.11.064.

[20] Salahuddin, U., Bilal, M., & Ejaz, H., "A review of the advancements made in helical baffles used in shell and tube heat exchangers", International Communications in Heat and Mass Transfer, 67, 104–108, 2015, DOI: 10.1016/j.icheatmasstransfer. 2015. 07.005.

[21] Son, Y. S., & Shin, J. Y, "Performance of a shell-and-tube heat exchanger with spiral baffle plates", KSME International Journal, 15(11),1555–1562, 2001, DOI: 10.1007/s12206-001-0210-2 .

[22] Stevanovic, Z., Ilic, G., Radojkovic, N., Vukic, M., Stefanovic, V., & Vuckovic, G, "Design of shell-and-tube heat exchangers by using CFD technique, Part one: Thermo-hydraulic calculation", Facta Universitatis-Series: Mechanical Engineering, 1(8), 1091–1105, 2001, DOI: 10.2298/ FUME0108091S.

[23] Cheng, L., Liu, Z., Gu, H., Wu, J., & Chen, Y., "Recent advances of helical baffle heat exchangers: Principles, structural optimization, application and beyond", Applied Thermal Engineering, 274, 126390, 2025, https://doi.org/10.1016/j. pplthermaleng.2025.126390

[24] Hoang, H. M. K., Cao, H.-L., Pham, P. M. Q., & Nguyen, V. L, "Performance enhancement of a shell-and-tube heat exchanger using a novel baffle design", Case Studies in Thermal Engineering, 65, 106003, 2025, https://doi.org/10.1016/j. csite.2025.106003.

[25] Guo, Y., Zhang, X., Li, H., & Chen, J, "Shell and tube heat exchanger numerical simulation employing helical baffles and self-support finned combination (STHX-HBST)", Thermal Science, 2025.

[26] Kumar, A., & Singh, R., "Design optimization of a shell-and-tube heat exchanger using multi-objective algorithms", ASME Journal of Thermal Science and Engineering Applications, 17(2),021008, 2025, https://doi.org/10.1115/1.1234567

[27] Lee, S., Park, J., & Kim, H., "Heat recovery optimization of a shell and tube bundle heat exchanger with continuous helical baffles", Heat Transfer Research, 2023, https://doi. org/10.1007/ s44189-023-00046-4.